JOURNAL OF CATALYSIS 51, 47–63 (1978)

The Desorption Kinetics of Water and Formic Acid from Ni(110) following Low-Temperature Adsorption

JOHN L. FALCONER* AND ROBERT J. MADIX†

* *Department of Chemical Engineering, University of Colorado, Boulder, Colorado 80309, and*
† *Department of Chemical Engineering, Stanford University, Stanford, California 94305*

Received August 30, 1976; revised September 6, 1977

The flash desorption of water and of formic acid and the flash decomposition of formic acid isotopes were studied on a clean Ni(110) surface for adsorption temperatures below −55°C. Most of the adsorbed water was found to be weakly bound to the surface and to desorb with first-order kinetics. An apparent surface phase transition was observed at high coverages which indicated interactions between adsorbed water molecules at high coverage. A fraction of the formic acid adsorbed at −60°C was very weakly bound to the surface and exhibited first-order desorption with a coverage-dependent activation energy. This coverage dependence was attributed to strong adsorbate–adsorbate interactions. The decomposition products for adsorption of a formic acid isotope, HCOOD, were H_2, CO_2, CO, and D_2O. The water product observed leaving the surface was formed from the acid hydrogens and was the result of a decomposition-limited reaction step. The kinetics to form water, which were zero order at high coverage and first order at low coverage, were explained in terms of an island mechanism in which formic acid adsorbed in a condensed phase. The decomposition to form CO_2 and H_2 proceeded at a faster rate than that observed from adsorption at 37°C. Also, the CO_2 and H_2 did not exhibit the narrow autocatalytic flash desorption peaks observed following 37°C adsorption. The same kinetic mechanism was operating at both adsorption temperatures but for low temperature adsorption the bare metal sites needed for reaction were created by desorption of the water product and thus the rate was faster at the lower adsorption temperature. For −60°C adsorption, all the CO product was desorption-limited.

INTRODUCTION

The flash decomposition of formic acid adsorbed on clean Ni(110) was shown previously to depend on the adsorption temperature (*1*). Studies of the decomposition of formic acid on this surface (*2*) indicated that following adsorption at 37°C the formic acid intermediate decomposed autocatalytically upon heating the nickel. Decomposition of formic acid following adsorption at −60°C indicated that water was a primary reaction product and that the adsorbed intermediate at 37°C was formic anhydride (*3*). In this work the decompositions of DCOOH and HCOOD following adsorption at −60 to −70°C were studied to determine the kinetics and mechanism of water formation and the changes in the formation of CO_2, CO, and H_2 products with adsorption temperature. Formic acid decomposition following low-temperature adsorption was also studied in order to explain the decomposition of formic acid in general. To complete the study of desorption properties of all reaction products the adsorption/desorption characteristics of water and formic acid were studied.

0021-9517/78/0511-0047$02.00/0

EXPERIMENTAL

The ultrahigh vacuum system employed contained AES-LEED four-grid optics and a quadrupole mass spectrometer (*1*). Flash spectra were obtained by flashing directly into the ionizer of the mass spectrometer to maximize the water signals, since the pumping speed of the system for water was extremely high. Because the vacuum chamber walls pumped the water, accurate values of pumping speeds could not be measured and absolute adsorption coverages for water could not be obtained.

The nickel surface was cleaned by bombarding with 300-V Ar ions and annealing at 500°C. Surface cleanliness was checked with AES and LEED (*1*). The surface was exposed to formic acid and water from the vapors above their respective solids at −45°C via a stainless steel syringe as described previously (*1*). The nickel sample was cooled from 500 to −55°C in approximately 5 min by conduction through a liquid nitrogen-cooled copper tube. Because of the relatively long cooling time, some background hydrogen adsorbed on the surface and obscured accurate determination of the product stoichiometry.

Formic acid-d (HCOOD) was purchased from International Chemical and Nuclear as 98% pure and 98% deuterated. NMR analysis showed at least 95% deuteration of the acid hydrogen. Many cycles of thawing, freezing, and pumping were needed to obtain a vapor pressure at −45°C which was independent of time, indicating purification of the acid. It was found necessary for reproducible results to flow the purified HCOOD through the stainless steel syringe for 30 min to exchange any H_2O and HCOOH on the walls of the gas feed system and syringe, so that pure HCOOD contacted the sample. The mass spectrum observed for HCOOD was similar to that of Ropp and Melton (*4*), but contained approximately 15% DCOOD. The purification of DCOOH was described earlier (*2*).

Triple-distilled H_2O was outgassed for several hours at −45°C until a vapor pressure was obtained which was independent of time. The vapor pressure was close to that of formic acid at −45°C. The mass spectrum for the purified water showed no detectable impurities.

RESULTS

H_2O Adsorption/Desorption

Because water was a reaction product for the decomposition of formic acid adsorbed at low temperature, water desorption curves were obtained for comparison. Flash desorption of water adsorbed on Ni(110) has not been previously reported, so a series of $H_2O/H_2O(-60)$[1] curves were obtained at different initial surface coverages. Figures 1 and 2 show a series of curves for water desorption with varying initial coverage. Though accurate coverages could not be obtained, comparison of the time required for saturation coverage of water with that required for formic acid saturation coverage (where each gas was flowed through the dosing needle with a known backing pressure) indicated that the initial sticking probability of water was of order unity at −60°C.

The two groups of water flash desorption peaks, the low-temperature peaks (α peaks), and the higher temperature peaks (β peaks) were observed to fill simultaneously, as seen in Figs. 1 and 2. At low initial coverages the α_2, β_1, β_2, and β_3 peaks were observed; the α_1 peak was not present. Though the three β peaks could not be easily separated, they appeared to fill in the order β_2, β_1, β_3. After the α_2 peak reached saturation, additional water exposure caused a slight depletion in the α_2 state and an increase in the α_1 peak coverage. The $H_2O/H_2O(-60)$

[1] A shorthand notation presented earlier for flash decomposition spectra will be employed. For example, the notation, $A(\alpha)/B(T)$, refers to the α state of desorbing gas A during a flash following adsorption of gas B at T°C.

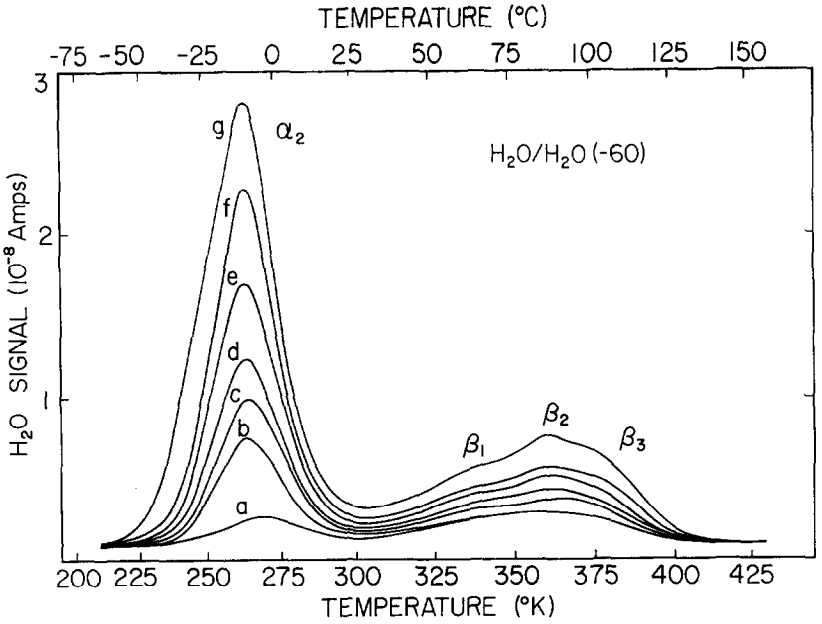

FIG. 1. $H_2O/H_2O(-60)$ flash desorption spectra for low coverages. Exposures in Langmuirs (1 L = 10^{-6} Torr sec): (a) 0.03, (b) 0.07, (c) 0.1, (d) 0.2, (e) 0.33, (f) 0.67, (g) 1.2.

peaks *all* appeared to be first order since their peak maximum locations did not shift with initial surface coverage.

When H_2O was desorbed from the nickel (110) surface some H_2 also desorbed. The H_2 peak corresponded to $H_2/H_2(-60)$, and the same size H_2 peak was observed when the nickel sample was moved away from the dosing syringe during adsorption so that H_2O did not impinge directly on the

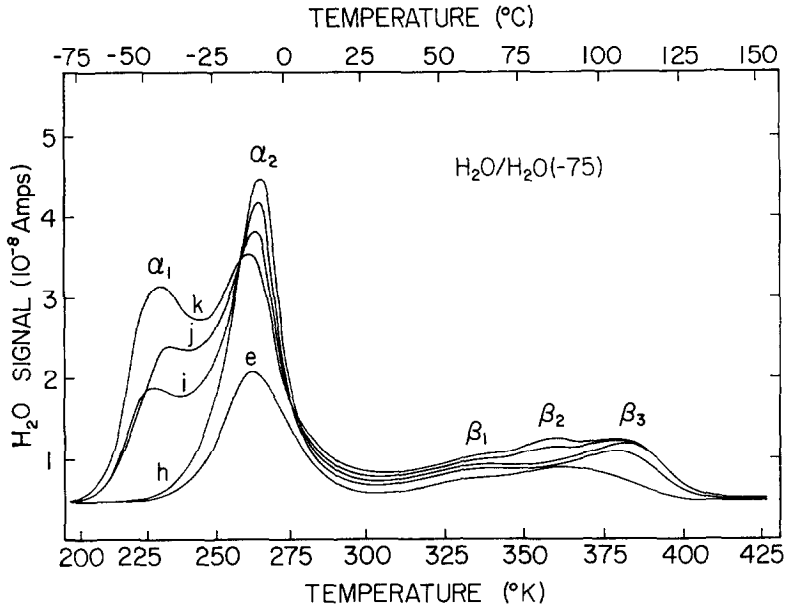

FIG. 2. $H_2O/H_2O(-75)$ flash desorption spectra for high coverages. Exposure in Langmuirs: (e) 0.33, (h) 2.7, (i) 6.7, (j) 10.0, (k) 13.3.

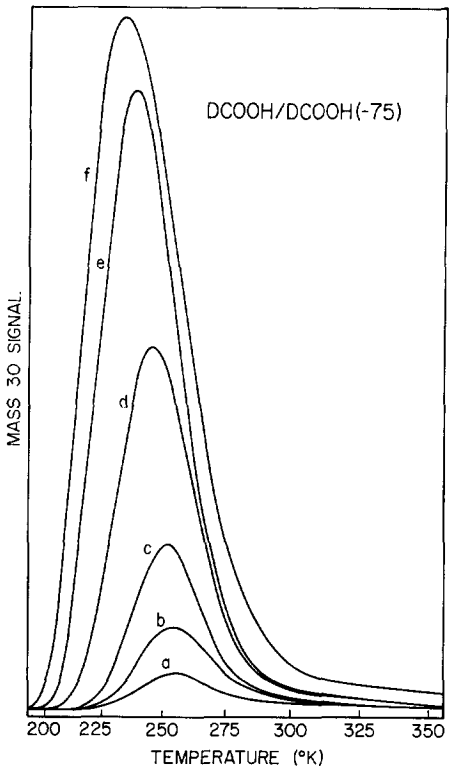

FIG. 3. DCOOH/DCOOH(−75) flash desorption spectra. Exposures in Langmuirs: (a) 0.5, (b) 1.0, (c) 2.0, (d) 6.7, (e) 13.3, (f) 26.7.

surface. Since the AES spectrum after several H_2O desorptions showed no oxygen on the surface, and because H_2 was the predominant background gas, the desorbing H_2 was attributed to coadsorption of H_2 from the background.

An estimate of the total water surface coverage was made by comparison of the H_2O/H_2O curve areas to curve areas from H_2O/DCOOH(−60) desorption. If the H_2O:CO product ratio was assumed to be 1:1 (*2*, *3*), then a $H_2O/H_2O(-60)$ saturation coverage of approximately 1×10^{15} molecules/cm^2 was obtained.

Formic Acid Desorption

Formic acid adsorbed at 37°C on clean Ni(110) decomposed completely; no formic acid desorbed upon subsequent heating. Following adsorption at −75°C, however, some formic acid was observed desorbing from the surface in a single peak below room temperature. The mass spectrometer was not easily calibrated for formic acid so that no determination of surface coverage corresponding to this peak was made. The desorption spectra were obtained by recording the mass 30 peak (DCO^+), the largest peak resulting from DCOOH cracking in the mass spectrometer ionizer. A series of DCOOH flash desorption curves for varying initial coverages of DCOOH at −75°C is shown in Fig. 3. As the formic acid exposure increased, the peak temperature decreased from −10°C for curve a to −36°C for curve f in Fig. 3. The DCOOH/DCOOH (−75) spectra did not reach saturation after 27 Langmuirs (L) of exposure (1 L = 10^{-6} Torr sec), though CO_2/DCOOH(−60) reached saturation with exposures of less than 10 L.

Formic Acid Decomposition

Water product. Formic acid-d (HCOOD) was adsorbed on clean Ni(110) at −60°C, and the decomposition products were observed for linear heating to 200°C. As reported previously (*3*) the only water product observed was D_2O; *no H_2O or HDO product was present.* A desorption peak at mass 18 was observed but it was shown to be due to the cracking of $D_2O(DO^+)$.

A series of D_2O/HCOOD(−60) curves for different initial coverages of HCOOD up to saturation is shown in Fig. 4. The water desorbed in three distinct peaks which were labeled, starting with the lowest temperature peak, as α_2, α_3, and β. The $D_2O(\alpha_2)$/HCOOD(−60) was similar to $H_2O(\alpha_2)/H_2O(-60)$; thus the above notation was used. The $D_2O(\alpha_2)$/HCOOD(−60) peak occurred at −13°C and the $D_2O(\beta)$/HCOOD(−60) peak occurred at approximately 106°C. The $D_2O(\alpha_3)$/HCOOD (−60) peak temperature *increased* with *increasing* initial coverage of HCOOD, changing from 16°C at a fractional coverage of D_2O of 0.06 to 54°C at saturation coverage.

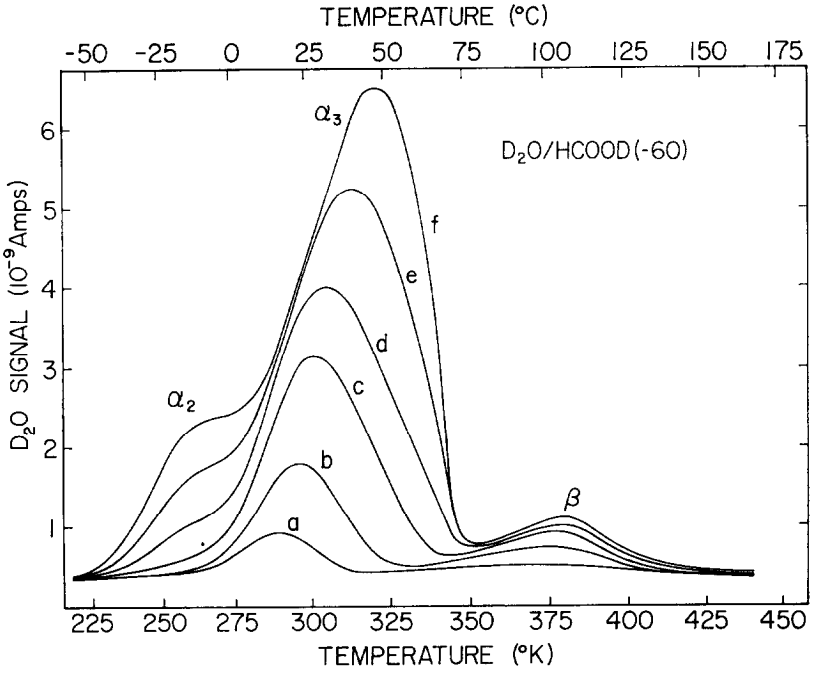

FIG. 4. D_2O/HCOOD(−60) flash decomposition spectra. Exposures in Langmuirs: (a) 0.02, (b) 0.03, (c) 0.16, (d) 0.33, (e) 0.67, (f) 1.33.

The $D_2O(\alpha_2)$/HCOOD(−60) and the $D_2O(\beta)$/HCOOD(−60) peaks may be due in part to D_2O impurity in the HCOOD. Their total area is approximately 15% of the total D_2O/HCOOD(−60) area, and their peak temperatures are close to those expected for D_2O/D_2O(−60), as estimated from the H_2O/H_2O(−60) desorption. The $D_2O(\beta)$ peaks may also be due to D_2O which formed during HCOOD adsorption and then remained adsorbed on the surface.

Similar to HCOOD decomposition, decomposition of DCOOH following adsorption at −60°C yielded H_2O as the only water product. A very small signal at mass 20 (less than 5% of the mass 18 signal) was due to D_2O from the DCOOD impurity. Figure 5 shows a series of H_2O/DCOOH (−60) flash decomposition spectra for different initial coverages. The H_2O/DCOOH(−60) spectra were similar to the D_2O/HCOOD(−60) spectra, but the $H_2O(\alpha_3)$ and $H_2O(\beta)$ peaks occurred at *higher* temperatures than the corresponding D_2O peaks at the same coverages. Figure 6 shows two sets of curves of H_2O/DCOOH (−60) and D_2O/HCOOD(−60) for comparison at low and high coverages. The curves were corrected for the difference in mass spectrometer sensitivities between H_2O and D_2O. It can be seen that the peak temperature for H_2O/DCOOH(−60) was higher than that for D_2O/HCOOD(−60), indicating that the rate constant for D_2O formation *exceeded* that for H_2O formation at a given temperature.

Carbon dioxide product. Formic acid decomposition to form CO_2 and H_2 following adsorption at −60°C occurred at a lower temperature than decomposition following adsorption at 37°C. Figures 7 and 8 show that CO_2/HCOOD(−60) was formed in two peaks. At low coverages the α_1 peak was formed; the peak temperature increased with initial coverage. The initial rate of decomposition was almost independent of coverage, indicative of a zero-order reaction. At higher exposures the α_2 peak was populated, and the α_1 peak decreased slightly in magnitude. The $CO_2(\alpha_2)$/

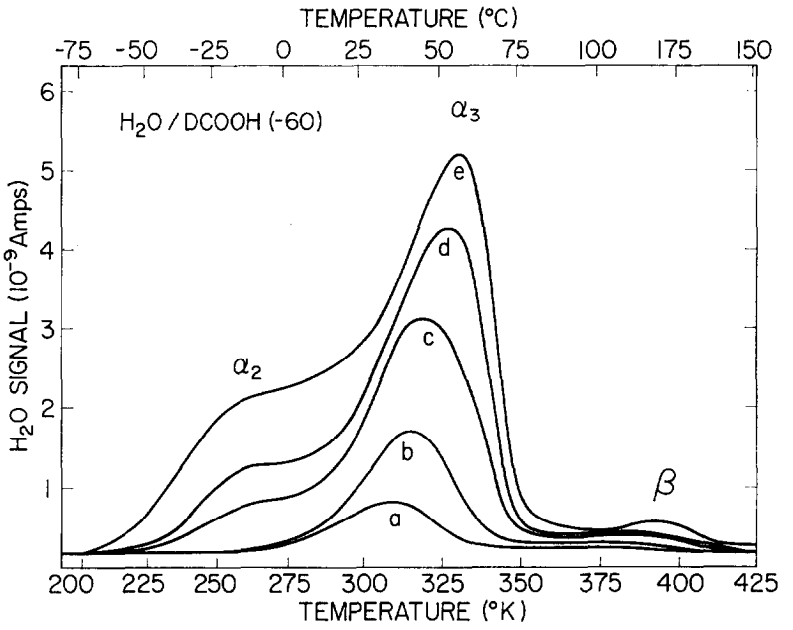

FIG. 5. $H_2O/DCOOH(-60)$ flash decomposition spectra. Exposure in Langmuirs: (a) 0.03, (b) 0.16, (c) 0.50, (d) 1.33, (e) 6.7.

HCOOD(−60) peak temperature was only slightly dependent on coverage. The α_2 peak showed a peak width at half-maximum of 11°C; for curve a the peak width of the α_1 state was 30°C. Due to isotope substitution the $CO_2(\alpha_2)/DCOOH(-60)$ peak

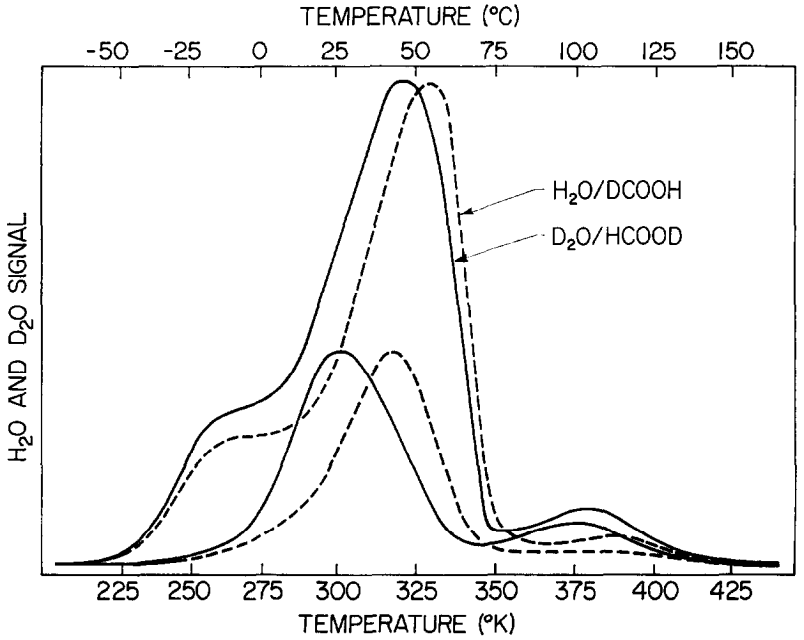

FIG. 6. Isotope shift for water product from formic acid decomposition at two coverages, 0.16 and 1.3 L of exposure. (——) $D_2O/HCOOD$; (– – –) $H_2O/DCOOH$.

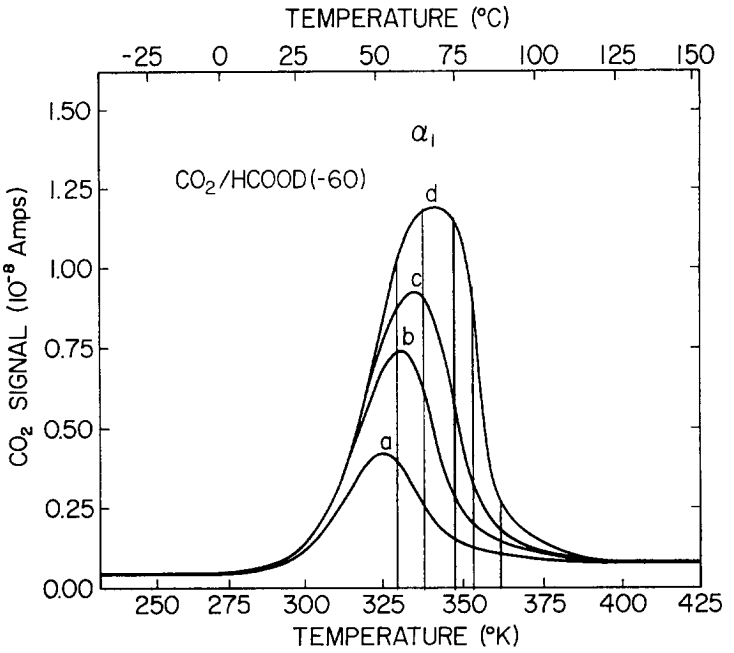

FIG. 7. CO_2/HCOOD(−60) flash decomposition spectra, low coverages. Exposures in Langmuirs: (a) 0.03, (b) 0.10, (c) 0.16, (d) 0.26. The light vertical lines indicate the temperature from which desorption isotherms were constructed.

had a peak temperature 13°C higher than the $CO_2(\alpha_2)$/HCOOD(−60) peak. Therefore, the $D_2(\alpha_2)$/DCOOH(−60) was formed at a slower rate than $H_2(\alpha_2)$/HCOOD (−60), though, as mentioned earlier, $D_2O(\alpha_2)$/HCOOD(−60) was formed at a

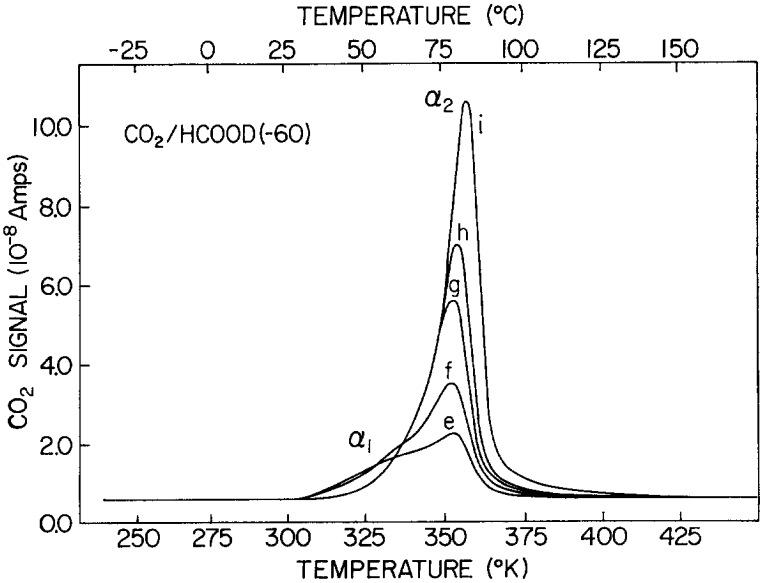

FIG. 8. CO_2/HCOOD(−60) flash decomposition spectra, high coverages. Exposures in Langmuirs: (e) 0.4, (f) 0.67, (g) 1.5, (h) 2.0, (i) 1.0.

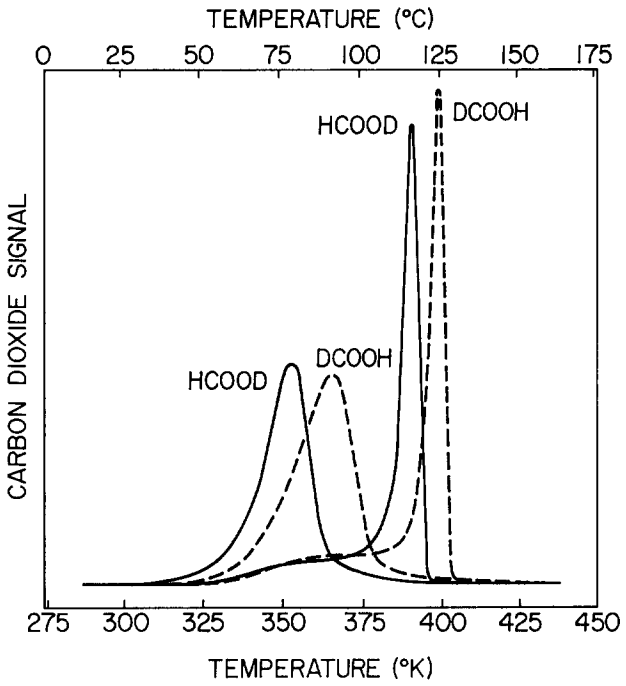

FIG. 9. Rates of carbon dioxide formation for 2 L of exposure of formic acid isotopes at −60°C (two peaks below 100°C) and at 37°C (two narrow peaks above 100°C).

faster rate than $H_2O/DCOOH(-60)$. This isotope shift is compared in Fig. 9 to the 8.5°C shift observed for 37°C adsorption. The amount of CO_2 formed following saturation coverage of formic acid at 37 and −60°C differed by less than 10%.

Both $H_2(\alpha_2)/HCOOD(-60)$ and $CO_2(\alpha_2)/HCOOD(-60)$ were formed at the same temperature with the same peak shape (*3*), indicating that H_2 and CO_2 were formed from the same intermediate. The details of the $H_2/HCOOD(-60)$ peak were obscured, however, by the presence of coadsorbed H_2 on the surface. Adsorption of DCOOH at −60°C permitted the corresponding $D_2/DCOOH(-60)$ curves to be observed without interference from coadsorbed H_2; they were essentially identical to $CO_2/DCOOH(-60)$ curves and thus are not reproduced here.

Effect of Adsorption Temperature

The narrow CO_2 and D_2 flash decomposition peaks indicative of the autocatalytic decomposition observed following DCOOH adsorption on clean Ni(110) at 37°C (*2*) were transformed to broader peaks with lower peak temperatures as the adsorption temperature was decreased. Figure 10 shows four $CO_2/DCOOH$ curves for adsorption temperatures, T_{ads}, from 42 to −75°C. For adsorption temperatures between +5 and −22°C the narrow β-peak disappeared and a broader peak formed at almost the same temperature as the small α peak observed for adsorption at 42°C (*2*). Though the peaks changed drastically with adsorption temperature, within an experimental error of 10% the CO_2 saturation surface coverage did not change.

The transition to lower peak temperatures may be continuous with adsorption temperature but it was not linear. Little change was observed upon lowering the adsorption temperature from +42 to +5°C, while changing the adsorption temperature from +5 to −22°C caused a major change in the peak temperature, shape, and

width. Further reduction of the adsorption temperature from −22 to −75°C caused little change in the decomposition curves.

Experiments involving sequential adsorptions at two temperatures before flashing were carried out to understand better the effect of adsorption temperature on the rate of decomposition. Attention was focused on the CO_2 product peak since it indicated the explosive properties of the decomposition. The results of these experiments are presented in Table 1.

The table shows that the adsorbed species, once formed at a given temperature, were stable until decomposition and desorption. When the Ni(110) surface was exposed to 2 L of HCOOD at −60°C, quickly heated to 55°C, cooled back to −60°C, and then flashed, the *only* change observed from CO_2/HCOOD(−60) was a decrease in product due to decomposition and desorption at 55°C. Thus, preheating the adsorbed species to 55°C did not produce the explosive decomposition to form CO_2. Likewise, cooling to −60°C before flashing following a 2-L exposure of the surface to HCOOD at 37°C did not effect the CO_2/HCOOD(37) explosive peak.

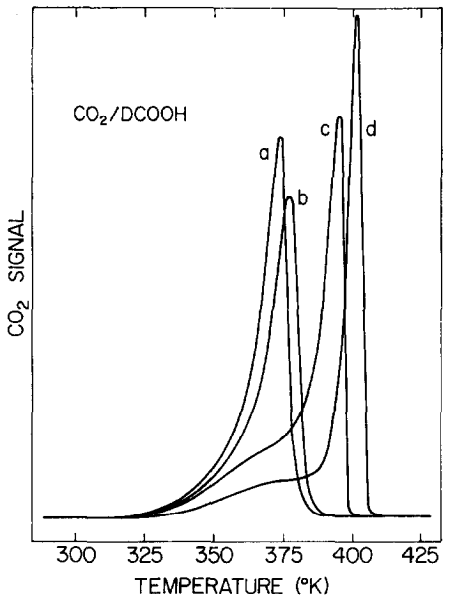

FIG. 10. CO_2/DCOOH flash decomposition spectra for 2 L of exposure at adsorption temperatures of (a) −75, (b) −22, (c) 5, and (d) 42°C.

TABLE 1

Effect of Adsorption Temperature on Decomposition

Adsorption of HCOOD	Flash desorption	
	Peak temperature (°C)	Peak width
(1) 2 L at 37°C; or 2 L at 55°C, cool to −60°C	116	Narrow
(2) 2 L at −60°C; or 2 L at −60°C, heat to 37°C, cool to −60°C	81	Broad
(3) 2 L at −60°C; then 2 L at 37°C	105	Narrow
(4) 1 L at −60°C, heat to 37°C; then 2 L at −60°C	82; 104	Broad; narrow

If, however, after 2 L of exposure of HCOOD at −60°C the sample was heated to 37°C and given an additional 2 L of exposure at 37°C, CO_2/HCOOD desorbed in a very *narrow* peak at 105°C (instead of the 116°C expected following 37°C adsorption or the 81°C expected for −60°C adsorption). The narrow peak at 105°C was similar to that observed with interrupted flashes reported earlier (*2*), indicating that a condensed phase of formic anhydride containing some bare metal sites was formed. If exposure to 1 L of HCOOD at −60°C was followed by heating the sample to 37°C, cooling, and then exposing to an additional 2 L of HCOOD at −60°C, a CO_2/HCOOD spectrum with two distinct peaks resulted, a narrow peak at 104°C and a broad peak at 82°C. The narrow peak amplitude was 3.0 times that of the broad peak but their areas were approximately the same.

Carbon monoxide product. Figure 11 shows CO/HCOOD(−60) decomposition curves at various coverages and a CO/HCOOD (37) curve at saturation for comparison. The CO(α_2) peaks were the same for both adsorption temperatures; they corresponded to CO(α_2)/CO(−60). The other CO peak observed for low-temperature

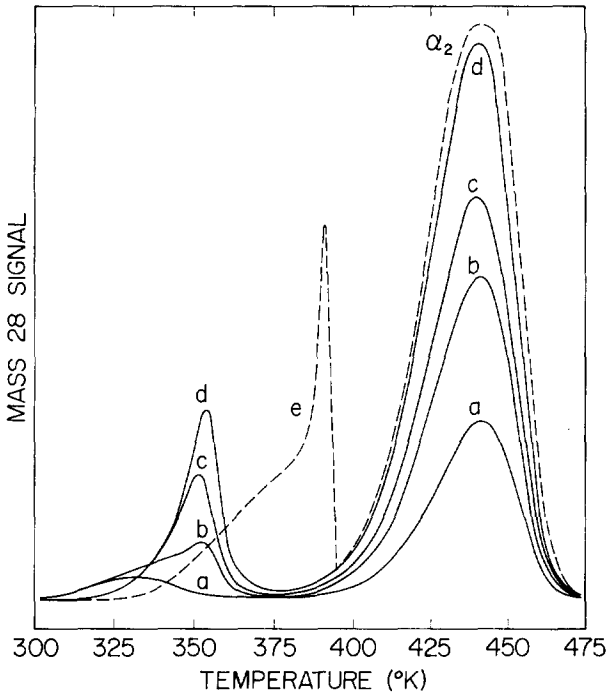

FIG. 11. CO/HCOOD(−60) Mass 28 flash decomposition spectra for HCOOD adsorption. Exposures in Langmuirs for adsorption at −60°C: (a) 0.16, (b) 0.5, (c) 2.0, (d) 3.0, and for adsorption at 37°C, (e) 3.0.

adsorption was due solely to mass spectrometer cracking of the CO_2/HCOOD (−60) peaks. Thus all CO product was observed as desorbing CO that had adsorbed on the surface following formic acid decomposition.

DISCUSSION

Water Flash Desorption

The most salient feature of the water flash desorption spectra was the α_2 peak; most of the water desorbed in the α_2 peak, so it characterized the desorption behavior of water from clean nickel (110) over a wide range of coverage. As seen in Figs. 1 and 2 the α_2 peak temperature did not shift significantly with coverage so that the desorption was apparently first order. However, the α_2 peak was not precisely described over the *entire* coverage range by a simple first-order expression because the peak width (width at half height) decreased at high initial coverage (curve h), though the peak temperature remained unchanged. The peak width for first-order desorption is independent of initial coverage.

The $H_2O(\alpha_2)/H_2O(-60)$ desorption curves in Fig. 1 were analyzed by several methods. For $\nu = 10^{13}$ sec^{-1}, a first-order activation energy of 15.5 kcal/mol was calculated using the equations of Redhead (*5*). The theoretical curves calculated from these values and shown as dashed lines in Fig. 12 are narrower than the experimental curves. A computed first-order curve which gave the same peak width and peak temperature corresponded to $\nu = 1.2 \times 10^{11}$ sec^{-1} and $E = 13.3$ kcal/mol. The leading edge of the $H_2O(\alpha_2)/H_2O(-60)$ peak was also analyzed by measuring the rates (N), coverages (θ), and temperatures (T) at a number of points along the low-temperature side of curve f in Fig. 1. A plot of ln (N/θ) against $1/T$ yielded a straight line, as expected for first-order desorption. The slope

corresponded to an activation energy of 14.2 kcal/mol, and the resulting pre-exponential factor was 8×10^{11} sec^{-1}.

The desorption curves in Fig. 1 for the α_2 peak were also analyzed using desorption rate isotherms by calculating the rates and coverages at selected temperatures over the desorption range for each initial coverage (*6*, *7*). Plots of $\ln N$ versus $\ln \theta$ yielded straight lines for each temperature selected. The slope of these lines corresponded to the order of the desorption. At high temperatures (i.e., on the decreasing part of the desorption curve) the slope gave a desorption order of unity. At lower temperatures n increased slightly (from 1.00 at 276 K to 1.13 at 259 K). Comparison to theoretically generated flash curves indicates that the activation energy for desorption decreased slightly with increased coverage (*6*). A plot of $\ln N$ against $1/T$ using points from the desorption rate isotherms at constant θ should be a straight line for first-order desorption with a coverage-dependent activation energy. However, it had significant curvature. Figure 1 indicates that, at low coverage, curve a had a higher peak temperature than the other curves for the α_2 peak. Apparently a small peak existed on the high temperature side of the α_2 peak. This probably caused the higher temperature side of the α_2 peak to appear broader than first order and caused the $\ln N$ versus $1/T$ plot to be nonlinear.

The activation energy obtained from the leading edge treatment was close to that obtained from the peak width and peak temperature. Thus the analysis confirmed that most of the water desorption was first order with an activation energy of 13 to 14 kcal/mol.

The remainder of the data for water desorption was complex and was not analyzed in detail. When the α_2 peak was subtracted from the high-coverage curves the resulting α_1 peaks were asymmetric, decreasing more slowly on the high-temperature side than even expected for *second-*

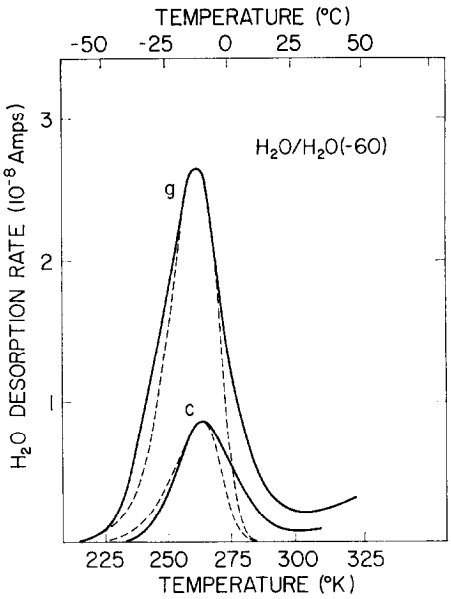

FIG. 12. Theoretical fit for $H_2O(\alpha_2)/H_2O(-60)$ desorption curves (c) and (g) of Fig. 1 for a first-order rate constant of $10^{13} \exp(-15{,}500/RT)$ sec^{-1}.

order desorption. This effect was also observed for the second-order desorption of D_2/HCOOD(−60) on Ni(110) (4 × 5)C (*8*) and DCOOH/DCOOH(−60) on nickel (110). A theoretical explanation for this slow tailing is known only for the case of second-order desorption (*9*). The important point to be emphasized with regard to the subsequent formic acid decomposition is that the major peaks for $H_2O/H_2O(-60)$ appeared below −10°C.

The formation of the α_1 peak with the slight depletion of the α_2 peak occurred above 0.6 coverage. This transition may indicate a surface ordering of the adsorbed water due to repulsive interactions. The α_2 peak saturated and then decreased as the phase transition occurred. If the same pre-exponential factor was assumed for the α_1 and α_2 peaks, the α_1 peak showed a binding energy 0.45 kcal/mol smaller than the α_2 state. This desorption energy for H_2O (α_1) of approximately 13.2 kcal/mol is close to the heat of solidification of water (12.24 kcal/mol) and indicates that the $H_2O(\alpha)$

peaks may result from a single condensed layer on the surface; multilayers were not observed.

Formic Acid Flash Desorption

As seen in Fig. 3, the peak temperature from formic acid desorption decreased from −18 to −36°C as the coverage increased, indicative of either desorption of order higher than one or of a first-order desorption with a coverage dependent activation energy. It was not likely that formic acid would dissociate at −70°C and then reassociate upon desorption without forming some reaction products, which were not observed. Thus to obtain second-order desorption it would be necessary to assume that formic acid molecules associated into dimers before desorption. However, a plot of ln $(C_o T_p^2)$ vs $1/T_p$ where C_o is the initial coverage and T_p is the peak temperature indicated that the desorption was not second order. For second-order desorption such a plot would be a straight line (*5*).

At selected temperatures desorption rates (N) and coverages (θ) were measured from each of the DCOOH/DCOOH(−70) curves in Fig. 3. Desorption rate isotherms were obtained by plotting N against $\ln \theta$ at constant temperature (*6*). On the high-temperature side of the flash desorption curves (corresponding to low surface coverages) the desorption rate isotherms indicated a desorption order of 1.05. At lower temperatures the apparent desorption order increased above 1.5 and the plots showed deviation from linearity. Theoretically generated desorption rate isotherms for first-order desorption with an activation energy that decreased linearly with coverage showed the same changes (*6*). Thus the decrease in peak temperatures with coverage for DCOOH desorption was apparently due to a first-order desorption with a coverage-dependent activation energy.

A first-order activation energy of 9.9 kcal/mol and a preexponential factor of 2.7×10^8 sec^{-1} were calculated from the peak temperature and half-width of curve b in Fig. 3. If the preexponential factor remained unchanged then the activation energy for curve f corresponded to 9.2 kcal/mol, which, for a linear change of E with θ, corresponded to $dE/d\theta$ equal to 2 kcal/mole. As observed for water desorption, these binding energy values are close to the heat of solidification for formic acid of 8.6 kcal/mol (*10*). Since the adsorption temperature was well below the 8.6°C freezing point of formic acid, the flash spectra apparently were due to evaporation of a condensed layer of formic acid; multilayers were not observed. However, the low value of the preexponential factor cannot be explained. It is a direct consequence of the width and non-first-order symmetry of the flash peak.

Formic Acid Decomposition

Formic acid flash decomposition following adsorption at −60°C was very similar in many ways to the flash decomposition spectra obtained following 37°C adsorption (*2*). In both cases CO_2, H_2, and CO were products of the reaction in about equal amounts; dihydrogen was formed from the carbon-bound hydrogen at the same temperature at which CO_2 formed; the CO formed in the reaction adsorbed on the surface and then desorbed at higher temperature. The two major differences observed following adsorption at lower temperature were: (1) The water product, formed from the acid hydrogens, could be observed; and (2) the CO_2 was not formed via an explosion mechanism, and it exhibited different curve shapes, desorption rates, and coverage dependence from that observed following adsorption at 37°C.

Water Formation

Formic acid adsorbed on Ni(110) at −60°C without decomposition. During the subsequent heating the water product was

observed to form exclusively from the acid hydrogens, necessitating the reaction of two formic acid molecules. Even for the HCOOD decomposition, if a significant number of H atoms were coadsorbed, the only water product observed was D_2O; there was no isotope mixing to form HDO or H_2O. As two formic acid molecules reacted to split an acid hydrogen from one and an OH group from the second to form water, a stable surface species was formed which had the chemical composition of formic anhydride (*3*) (an otherwise unstable and unobserved molecular species). A comparison of the flash desorption curves for $H_2O/H_2O(-60)$ and $H_2O/DCOOH(-60)$ in Figs. 1 and 5, respectively, indicated that most of the $H_2O/DCOOH(-60)$ was the result of a decomposition-limited (not desorption-limited) reaction step, since the major $H_2O/H_2O(-60)$ peaks appeared at −10°C, a much lower temperature than that at which the $H_2O/DCOOH(-60)$ peaks appeared (35°C and above). Though the reaction to form water involved the interaction of two formic acid molecules to form another species, the decomposition spectra were *not* second order. The major water peak, the $H_2O(\alpha_3)/DCOOH(-60)$ peak, shifted to *higher* temperature with increasing initial coverage, indicative of a reaction order less than one. The smaller $H_2O(\alpha_2)/DCOOH(-60)$ peaks corresponded to $H_2O(\alpha_2)/H_2O(-60)$, which indicated that either some water was formed at low temperatures and was desorption-limited or that the formic acid contained a water impurity which simultaneously adsorbed on the surface.

The apparent fractional order for formic acid decomposition to form water may have been due to a zero-order reaction initially, which increased in order as the coverage decreased. Indeed, for $D_2O(\alpha_3)/HCOOD(-60)$ desorption, which was less obscured by the $D_2O(\alpha_2)$ peak than was $H_2O(\alpha_3)/DCOOH(-60)$ by the $H_2O(\alpha_2)$ peak, the initial desorption rates for different initial coverages were almost identical, indicative of zero-order desorption at high coverages. Also, a plot of the logarithm of rate versus inverse temperature for the leading edge of the $D_2O(\alpha_3)/HCOOD(-60)$ curves yielded a straight line which corresponded to a zero-order activation energy of 13.8 kcal/mol and a preexponential factor of 1×10^9 C_{sat} sec^{-1}. C_{sat} is the coverage in molecules per square centimeter at saturation. Desorption rate isotherms for $D_2O(\alpha_3)/HCOOD(-60)$ yielded straight lines with slopes decreasing from $n = 1.06$ at 330 K to 0.62 at 307 K. At lower temperatures the desorption rates were almost independent of coverage, corresponding to $n = 0$. The desorption rate isotherms indicated that the reaction changed from zero order at high coverage to first order at low coverage. This apparent change in order has been explained by the island-type mechanism discussed by Arthur and Cho (*11*), Arthur (*12*), and McCarty and Madix (*13*). Apparently equilibrium existed between condensed and rarefied phases of formic acid on the surface, with the condensed phase acting as a reservoir for the formic acid decomposing in the rarefied phase. The local concentration in both phases remained unchanged, and thus decomposition in the rarefied phase appeared zero order. However, equilibrium could not be maintained throughout the entire course of the reaction and eventually dissociation from the edges of the condensed phase or diffusion of the species away from the island perimeter became rate limiting, and the decomposition showed a coverage dependence. As explained elsewhere (*11–13*), for this occurrence the rate could transform to half order or first order so that the peak temperature increased with increased initial coverage, as observed for water formation.

Figure 6 shows a comparison between the $H_2O/DCOOH(-60)$ and $D_2O/HCOOD(-60)$ peaks at two different coverages. At both low and high coverages the H_2O peak had a higher peak temperature than the

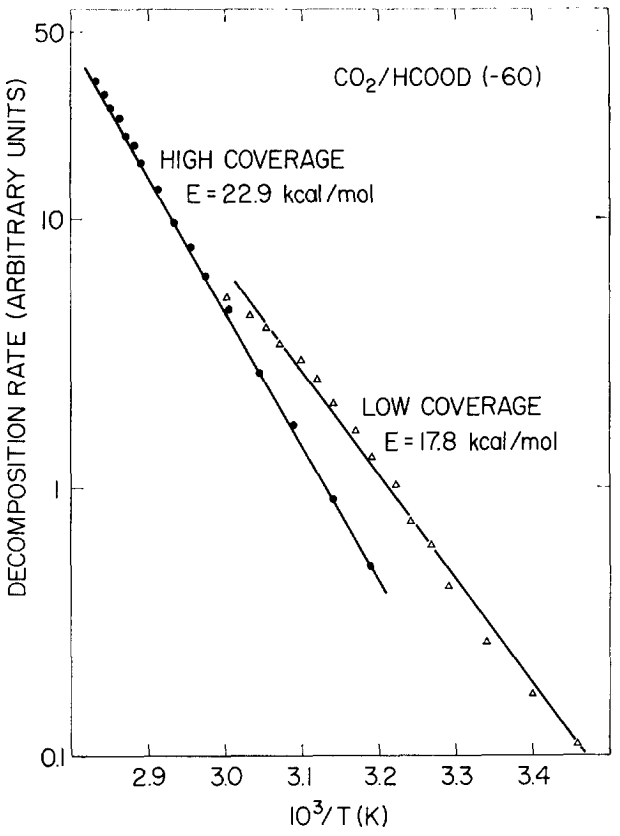

FIG. 13. Rate of decomposition versus inverse temperature for leading edge of CO_2/HCOOD(−60) curves of Fig. 7 (low coverage) and Fig. 8 (high coverage).

D_2O peak, contrary to the isotope effect that might be expected if the rate-determining step was O–H bond breaking. However, without detailed knowledge of the transition state on the surface, it is not possible to calculate theoretically the expected isotope effect for such a small effect. It is noteworthy that such effects can easily be detected in these studies.

Carbon Dioxide Formation

The shift in CO_2 decomposition peaks to lower temperature with decreased adsorption temperature indicated that decomposition occurred more readily as the adsorption temperature was lowered. The experiments summarized in Table 1 indicate that densely packed islands of formic anhydride were not formed if the formic acid adsorbed at −60°C was subsequently heated to +55°C. The flash to 55°C desorbed all the water product but the resultant adsorbed species did not decompose in a narrow desorption peak. Apparently the formic anhydride thus formed was not present in densely packed islands and a sufficient number of unoccupied metal sites were present to permit the decomposition reaction to occur nonautocatalytically at lower temperatures. If the surface was given formic acid exposure at 37°C subsequent to adsorption at −60°C and a flash to 55°C, an autocatalytic peak *was* seen. This peak corresponded to the interrupted flashes reported previously (*2*). In the interrupted flash experiments, bare sites were introduced into the islands by preflashing following adsorption at 37°C. The series of experiments in Table 1 are all consistent with the fact that, when the

water product was formed following adsorption at −60°C, it created a large number of bare metal sites for the decomposition of the anhydride. Thus the flashes at different adsorption temperatures were similar to interrupted flashes and a similar decomposition reaction step to form CO_2 was operating at both low and high adsorption temperatures.

However, the CO_2/HCOOD(−60) curve shapes and their dependence on initial coverage were quite different from the CO_2 curves obtained after 37°C adsorption of HCOOD. The leading edge of the low coverage curves in Fig. 7 was independent of coverage, indicative of a zero-order reaction. Figure 13 shows a plot of desorption rate versus inverse temperature for this leading edge. An activation energy of 17.8 kcal/mol was obtained for the α_1 peaks, though the scatter was sufficient that this plot alone was not a good indication of a zero-order reaction. The temperature of the peak maximum increased as the initial coverage increased, indicative of a desorption process with order between zero and one. Also, curves with a higher surface coverage had a lower desorption rate for the same temperatures for the α_1 peaks (curves e, f, and g in Fig. 8).

Desorption rate isotherms obtained for the low-coverage $CO_2(\alpha_1)$ curves in Fig. 7 are shown in Fig. 14. Each isotherm was not fit by a straight line but was very well fit by two intersecting straight lines. For very low coverages, the reaction order increased with decreasing temperature, while, for higher coverage, *but still a small fraction of the total CO_2 coverage*, the reaction order decreased for lower temperature. No simple kinetic explanation is available for this complicated transition in reaction orders.

Constant temperature desorption for the $CO_2(\alpha_2)$/HCOOD(−60) peak indicated this peak was not autocatalytic. The peak temperature did not change much with initial coverage indicating that the reaction was probably first order. However, the curves g, h, and i in Fig. 8 all appear to have the same initial rise. In fact a plot of the logarithm of the initial decomposition rate (height of curve in Fig. 8) as a function of temperature gave an *extremely* good fit

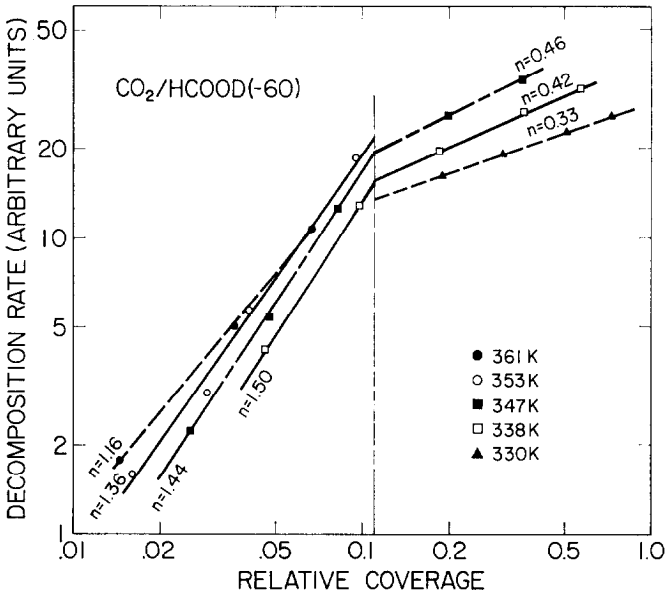

FIG. 14. Desorption rate isotherms at five temperatures for low-coverage CO_2/HCOOD(−60) curves in Fig. 7.

to a zero-order activation energy of 22.9 kcal/mol. This fit was obeyed for a change of almost two orders of magnitude in decomposition rate, a strong indication that the decomposition was initially zero order. The corresponding preexponential factor was $1 \times 10^{14}\ C_{sat}\ sec^{-1}$. However, the weak dependence of peak temperature on initial coverage at high exposure indicated that a transition occurred to first order. The $CO_2(\alpha_2)$ curves in Fig. 8 were also analyzed by plotting desorption rate isotherms at a number of temperatures. These plots of ln N versus ln θ indicated that the reaction was zero order at high coverages and approached an order greater than one at lower coverages.

The $CO_2(\alpha_2)$/DCOOH(−60) peak temperature at high coverage was very close to the $CO_2(\alpha)$/DCOOH(37) peak at saturation, as seen in Fig. 10. Previously (*2*), the $CO_2(\alpha)$/DCOOH(37) was attributed to decomposition in a rarefied phase where the concentration of bare metal sites was large. The similarity between the two peaks may indicate that the $CO_2(\alpha_2)$ peak resulting from low-temperature adsorption had a large number of unoccupied metal sites available for reaction and thus the two peaks resulted from the same elementary step. The $CO_2(\alpha)$/DCOOH(37) peak was not studied extensively and thus more detailed comparisons are not possible.

At *both* low and high exposures to HCOOD the decomposition of the anhydride to form CO_2 *initially* proceeded with zero-order kinetics. That is, zero-order behavior did not appear to be related explicitly to high coverage; rather it occurred at temperatures where adsorbed formic acid was still reacting to form water. Apparently, the surface reaction to form water interfered with the subsequent decomposition of the anhydride to form CO_2, possibly because of a competition for bare metal sites needed for the decomposition. Thus, zero-order behavior was observed in the initial stages of decomposition because the reaction to *form* the anhydride impeded site formation *within* the condensed phase, and in the initial stage of decomposition molecules on the periphery of the islands decompose to CO_2 by zero-order kinetics.

CONCLUSIONS

The low-temperature adsorption/desorption behavior of water and of formic acid was studied on clean Ni(110) by flash desorption. Water was found to be weakly bound to the surface with an activation energy for desorption of 13.7 kcal/mol. Similarly, a fraction of the adsorbed formic acid was weakly bound to the surface and desorbed unreacted with a coverage-dependent activation energy of approximately 9 kcal/mol. Both water desorption and formic acid desorption were found to be first order.

Most of the formic acid which was adsorbed at −60°C decomposed when the surface was heated. The decomposition mechanism for low-temperature adsorption was consistent with the previously reported flash decomposition results for adsorption at 37°C. The reaction steps are summarized below for decomposition of formic acid-d (HCOOD).

Adsorption at −60°C

$$HCOOD(g) \rightarrow [HCOOD]_{\text{condensed phase}} \quad (1)$$

Flash Decomposition

$$[HCOOD]_{\text{condensed phase}} \rightarrow HCOOD(g) \quad (2)$$

$$[HCOOD]_{\text{condensed phase}} \rightarrow [HCOOD]_{\text{rarefied phase}} \quad (3)$$

$$2[\mathrm{HCOOD}]\text{rarefied phase} \rightarrow (\mathrm{HCOOOCH})_{ads} + \mathrm{D_2O(g)} \quad (4)$$

$$(\mathrm{HCOOOCH})_{ads} \rightarrow \mathrm{CO_2(g)} + 2\mathrm{H}_{ads} + \mathrm{CO}_{ads} \quad (5)$$

$$2\mathrm{H}_{ads} \rightarrow \mathrm{H_2(g)} \quad (6)$$

$$\mathrm{CO}_{ads} \rightarrow \mathrm{CO(g)} \quad (7)$$

At $-60°C$ formic acid adsorbed without reaction on the surface in a condensed phase. Some of the formic acid desorbed without decomposition. Because the condensed phase acted as a reservoir for a rarefied phase in which decomposition occurred, the formation of the water product was zero order at high coverage and first order at lower coverage. The formic anhydride resulting from reaction (4) decomposed to form CO_2 and H_2 as the sample temperature was raised. The reaction rate was proportional to the concentration of anhydride and the concentration of unoccupied metal sites. Since the decomposition to form water created bare metal sites, the anhydride decomposition did not appear autocatalytic. Since reactions (3), (4), and (5) were occurring simultaneously during part of the decomposition, reaction (5) appeared initially zero order due to the influence of reactions (3) and (4). The subsequent reaction (6) was rapid, and reaction (7) occurred as the sample was heated to higher temperatures.

REFERENCES

1. McCarty, J., Falconer, J., and Madix, R. J., *J. Catal.* **30**, 235 (1973).
2. Falconer, J. L., and Madix, R. J., *Surface Sci.* **46**, 473 (1974).
3. Falconer, J. L., and Madix, R. J., *Surface Sci.* **51**, 546 (1975).
4. Ropp, G. A., and Melton, C. E., *J. Amer. Chem. Soc.* **80**, 3509 (1958).
5. Redhead, P. A., *Vacuum* **12**, 203 (1962).
6. Falconer, J. L., and Madix, R. J., *J. Catal.* **48**, 262 (1977).
7. Christmann, K., Ertl, G., and Pignet, T., *Surface Sci.* **54**, 365 (1976).
8. Abbas, N. M., and Madix, R. J., *Surface Sci.* **62**, 739 (1977).
9. Schmidt, L. D., *Catal. Rev. Sci. Eng.* **9**, 115 (1974).
10. "Handbook of Chemistry and Physics." R. C. Weast, Ed., CRC Press, Cleveland, Ohio, 1973.
11. Arthur, J. R., and Cho, A. Y., *Surface Sci.* **36**, 641 (1973).
12. Arthur, J. R., *Surface Sci.* **38**, 394 (1973).
13. McCarty, J. G., and Madix, R. J., *Surface Sci.* **54**, 210 (1976).